

Reaction of 2,4,6-Triazido-1,3,5-triazine with Triphenylphosphane. Syntheses and Characterization of the Novel 2-Triphenylphosphanimino-4-azidotetrazolo[5,1-*a*]-[1,3,5]triazine and 2,4,6-Tris(triphenylphosphanimino)-1,3,5-triazine

Elmar Kessenich, Kurt Polborn,[†] and Axel Schulz*

Department Chemie, Ludwig-Maximilians-Universität München, Butenandtstrasse 5-13 (Haus D), D-81377 München, Germany

Received May 19, 2000

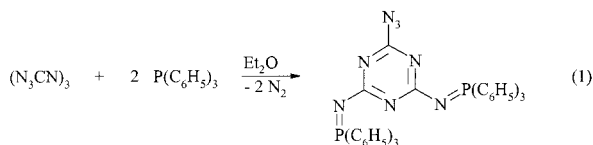
2-Triphenylphosphanimino-4-azidotetrazolo[5,1-*a*]-[1,3,5]triazine (**6**) was obtained by reaction of 2,4,6-triazido-1,3,5-triazine (**1**) with 1 equiv of triphenylphosphane. Raman and X-ray data revealed that only one azide group formed a tetrazole ring system whereas the second azide group did not undergo ring closure. To investigate the equilibrium between the tetrazole isomer and the open-chain azide structure for these and related species, ³¹P NMR studies were carried out. The obtained spectra displayed an equilibrium between the tetrazole and the open-chain azide isomers. 2,4,6-Tris(triphenylphosphanimino)-1,3,5-triazine (**4**) was prepared by treatment of **1** with 3 equiv of triphenylphosphane, and its X-ray structure is discussed. On the basis of PM3 semiempirical and density functional calculations, the reaction of **1** with triphenylphosphane was studied. The thermodynamics of different isomerization reactions and the activation barriers to cyclization were estimated.

Introduction

Staudinger and Meyer¹ found out that phenyl azide reacts with triphenylphosphane in anhydrous ether to form a phosphazide (C₆H₅–NNN–P(C₆H₅)₃). They postulated the formation of unstable intermediates that cannot be isolated at room temperature because they spontaneously emit nitrogen to form triphenylphosphanophenylimine.

As early as 1907, W. Kesting investigated the reaction of 2,4,6-triazido-1,3,5-triazine (**1**) with triphenylphosphane.² Ever since then there has been considerable interest in the reactivity and explosive character of **1** and its derivatives.³

According to the following reaction



the formation of 2,4-bis(triphenylphosphanimino)-6-azido-1,3,5-triazine (**3**) was suggested which, despite the remaining azide group, showed neither shock nor heat sensitivity.

Since the azido group is attached to a C atom adjacent to an annular nitrogen, it may spontaneously cyclize to give a tetrazole

ring or an equilibrium mixture of both forms. This type of azido–tetrazole isomerization has been the subject of many studies⁴ and was defined by Huisgen as a 1,5-dipolar cyclization.⁵ In most cases, azido–tetrazole equilibria were observed in solution; in some cases, this phenomenon was also observed in the melt.^{4,6} The electronic reorganization along the azido–tetrazole isomerization pathway has been discussed by several groups.^{7–9} The population of azido and tetrazole forms depends strongly on the solvent, temperature, and nature of the substituents.¹⁰

Recently we reported on the characterization of 2,4-bis(triphenylphosphanimino)tetrazolo[5,1-*a*]-[1,3,5]triazine (**7**).¹¹ In this study we demonstrate that the final products of the reaction of **1** with triphenylphosphane and their distribution strongly depend on the reaction conditions, stoichiometry, and temperature. Depending on the stoichiometry, different products are formed that could be isolated and characterized.

Results and Discussion

Experimental Characterization. By addition of 1 equiv of triphenylphosphane to a solution of **1** in ether, initially a yellow-

* To whom correspondence should be addressed. E-mail: lex@cup.uni-muenchen.de. Fax: +49-89-21807492. Phone: +49-89-21807763.

[†] Performed X-ray structure analysis.

- (1) Staudinger, H.; Meyer, J. *Helv. Chim. Acta* **1919**, 635.
- (2) Kesting, W. *J. Prakt. Chem.* **1923**, 105 (2), 242.
- (3) (a) Bragg, N. *Nature* **1934**, 134, 138. (b) Knaggs, I. *Proc. R. Soc. London* **1935**, A150, 576. (c) Wöhler, L. *Angew. Chem.* **1922**, 35, 545. (d) Koenen, H.; Ide, K. H.; Haupt, W. *Explosivstoffe* **1958**, 10, 223. (e) Kast, H.; Haid, A. *Angew. Chem.* **1925**, 38, 43. (f) Beck, W.; Bauder, M. *Chem. Ber.* **1970**, 103, 583. (g) Müller, J. *Z. Naturforsch. B* **1979**, 34, 437. (h) Shearer, J.; Bryant, J. I. *J. Chem. Phys.* **1968**, 48 (3), 1138.

- (4) Tišler, M. *Synthesis* **1974**, 123–136 and references therein.
- (5) Huisgen, R. *Angew. Chem.* **1968**, 80, 329; *Angew. Chem., Int. Ed. Engl.* **1968**, 7, 321.
- (6) Wentrup, C. *Tetrahedron* **1970**, 26, 4969.
- (7) Cubero, E.; Orozco, M.; Luque, F. J. *J. Am. Chem. Soc.* **1998**, 120, 4723.
- (8) Burke, L. A.; Elguero, J.; Leroy, G.; Sana, M. *J. Am. Chem. Soc.* **1976**, 98, 1685.
- (9) Kurz, D.; Reinhold, J. *J. Mol. Struct.: THEOCHEM* **1999**, 492, 187.
- (10) (a) Butler, R. N. *Comprehensive Heterocyclic Chemistry*; Katritzky, A. R., Rens, C. W., Scriven, E. F. V., Eds.; Pergamon: Oxford, U.K., 1996; Vol. 4, p 621. (b) Elguero, J.; Claramunt, R. M.; Summers, A. J. H. *Adv. Heterocycl. Chem.* **1978**, 22, 183. (c) Lieber, E.; Minnis, R. L.; Rao, C. N. R. *Chem. Rev.* **1965**, 65, 377.
- (11) Kessenich, E.; Klapötke, T. M.; Polborn, K.; Schulz, A. *Eur. J. Inorg. Chem.* **1998**, 2013.

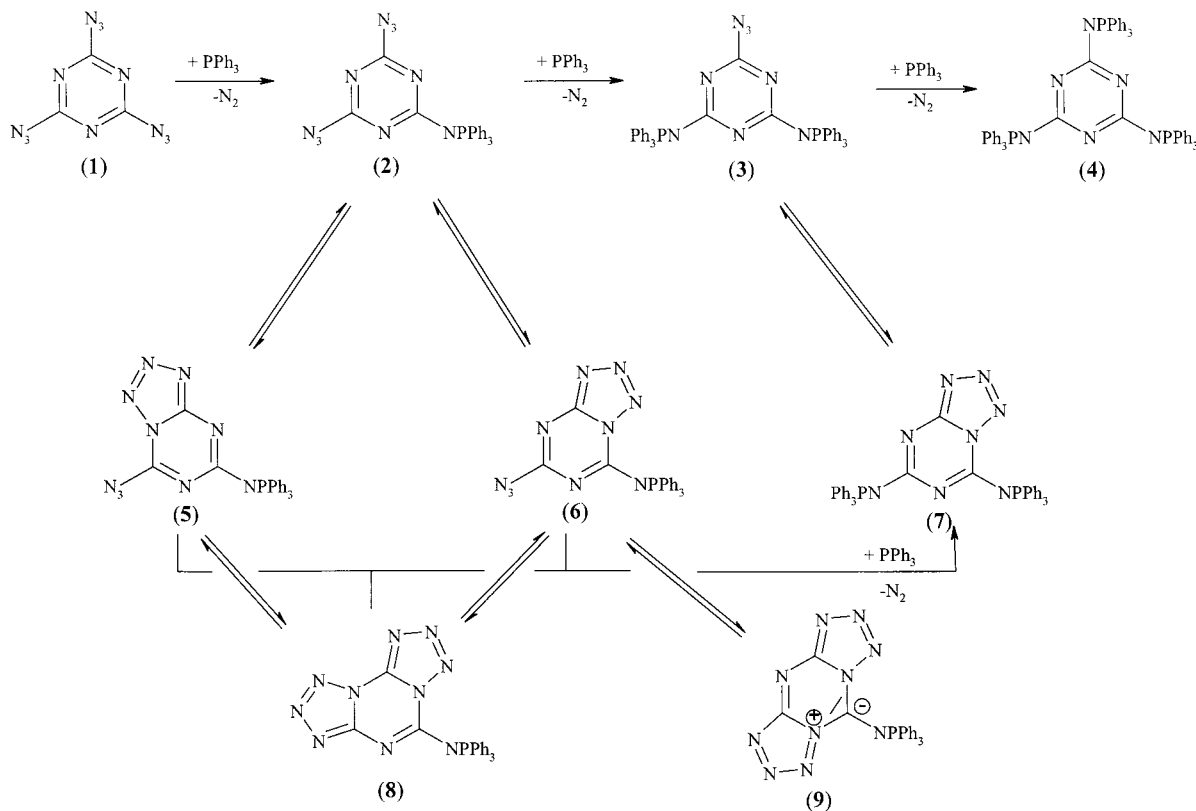


Figure 1. Diagram of the reaction PPh_3 with **1** and the equilibria between the tetrazole and the azide isomers.

Table 1. ^{31}P NMR Shifts in CDCl_3

compound	δ [ppm] ^a	rel intensity
PPh_3	-4.6	
6 ^b	24.7	2.6
2 ^b	21.6	1
6 ^c	24.9	56
2 ^c	21.1	1
7	21.1	5
7	16.7	5
3	15.7 (br)	1
4	12.3	

^a 25 °C. ^b Temperature-dependent ^{31}P NMR experiment: 60 °C 1.4:1; 50 °C 1.6:1; 40 °C 1.8:1; 30 °C 2.1:1; 20 °C 2.6:1; 10 °C 2.9:1; 0 °C 2.9:1; -10 °C 3:1 (at lower temperature precipitation occurs). ^c Temperature-dependent ^{31}P NMR experiment: 30 °C 50:1; 50 °C 36:1; 80 °C 12:1; 120 °C 6:1; 150 °C 5:1 in $[\text{D}_6]\text{DMSO}$.

green intermediate is formed, thought to be due to the formation of $\text{R}-\text{NNN}-\text{P}(\text{C}_6\text{H}_5)_3$ (R = diazido-triazine moiety). This adduct has only fleeting existence and decomposes by giving off N_2 , resulting in the formation of monophosphanimino-diazide (**2**) (Figure 1). The reaction was estimated to be exothermic ($\Delta E[\text{B3LYP}/6-31\text{G}(\text{d})//\text{PM3}] = -72$ kcal/mol; see Computational Methods). ^{31}P NMR data suggest the partial transformation of **2** into the tetrazole isomers **5** or **6** in an equilibrium reaction. The formation of **5** is less likely because **6** is stabilized by about 7.5 kcal/mol ($\text{B3LYP}/6-31\text{G}(\text{d})//\text{PM3}$). The ring formation $\mathbf{2} \rightarrow \mathbf{6}$ represents a true equilibrium reaction ($K_{\text{exp}}(298 \text{ K}, \text{CDCl}_3) = 2.6$; see Tetrazole vs Azide and Table 1). Depending on the level of theory the estimated Gibbs free energy is ± 2 kcal/mol ($\Delta E[\text{B3LYP}/6-31\text{G}(\text{d})] = -0.25$ kcal/mol; $\Delta E[\text{B3LYP}/6-31\text{G}(\text{d})//\text{PM3}] = 1.31$ kcal/mol), which is in good agreement with the experimental value of -0.57 kcal/mol derived from ^{31}P NMR experiments.¹²⁻¹³

The presence of one remaining azide group in **6** was deduced from Raman and IR spectroscopy. Bands at 2146 cm^{-1} (Raman,

$\nu_{\text{as}}(\text{NNN})$, weak) and 2150 cm^{-1} (IR, $\nu_{\text{as}}(\text{NNN})$, strong) assigned to the characteristic asymmetric stretching vibration of the azide group in combination with the molecular peak (mass spectrometry) supported this assumption. X-ray structure analysis of suitable single crystals confirms the formation of the novel 2-triphenylphosphanimino-4-azidotetrazolo[5,1-*a*]-[1,3,5]triazine (**6**) in the solid state. After crystals of **6** were dissolved, the recorded NMR spectra again showed two signals with an intensity ratio of 2.6:1 (tetrazole/azide), which can be explained by an equilibrium between the tetrazole isomer **6** and the open-chain azide structure **2**. The two ^{31}P NMR signals at $\delta = 24.7$ and $\delta = 21.6$ were observed at 25 °C. However, the equilibrium depends on the temperature.^{4,10,14} The intensity ratio changes to 1.4:1 when the temperature is raised to 60 °C and returns to 2.6:1 upon cooling. Further cooling to -50 °C leads to a decrease of the azide intensity and finally to precipitation of the tetrazole (**6**). Cleavage of the tetrazole ring is generally an endothermic process in solution, which explains that higher temperatures favor the azido species.^{10b,15} Furthermore, the isomerism is solvent-dependent. Polar solvents favor the tetrazole form, and nonpolar solvents, the azido species. The assignment of the ^{31}P , ^{15}N , and ^{13}C NMR signals for the tetrazole was deduced from measurements in $[\text{D}_6]\text{DMSO}$ and from comparison with literature data.¹⁶ The assignment was possible because in DMSO a large excess of the tetrazole was observed (intensity ratio 56:1; see Tables 1 and 2).

(12) (a) It should be noted that the computation was carried out for single, isolated (gas-phase) molecules. Therefore, small differences between gas-phase and solid-state or solution data are expected. (b) Klapötke, T. M.; Schulz, A. *Quantum Chemical Methods in Main-Group Chemistry* (with an invited chapter by Harcourt, R. D.); Wiley & Sons: Chichester, 1998.

(13) For this type of isomerization the $\Delta G(298 \text{ K})$ value should not differ much from the $\Delta E(0 \text{ K})$ value.

(14) Patai, S. *The Chemistry of the Azido Group*; Wiley: New York, 1971.

(15) McEwan, W. S.; Rigg, M. W. *J. Am. Chem. Soc.* **1951**, *73*, 4725.

Table 2. ^{13}C and ^{15}N NMR Resonances^a of **6** (δ in ppm, [D6]DMSO)

$^{13}\text{C}/^{15}\text{N}^b$		$^{13}\text{C}/^{15}\text{N}^b$	
N1	-266.3 (d, $^1J_{\text{NP}} = 32.5$ Hz)	N9/N10	-142.5
N2	-181.2 (d, $^3J_{\text{NP}} = 6.5$ Hz)		-144.2
N3	-192.4	C19	151.6 (d, $^2J_{\text{CP}} = 1.6$ Hz)
N4	-79.1	C20	162.9 (d, $^4J_{\text{CP}} = 1.5$ Hz)
N5	17.0	C21	158.5 (d, $^4J_{\text{CP}} = 1.5$ Hz)
N6	-35.1	1C _{phenyl}	124.5 (d, $^1J_{\text{CP}} = 102.6$ Hz)
N7	-151.1 (d, $^3J_{\text{NP}} = 11.2$ Hz)	2C _{phenyl}	129.3 (d, $^2J_{\text{CP}} = 13.0$ Hz)
N8	-265.4	3C _{phenyl}	132.9 (d, $^3J_{\text{CP}} = 10.8$ Hz)
		4C _{phenyl}	133.7 (d, $^4J_{\text{CP}} = 3.0$ Hz)

^a For numbering of the atoms see Figure 4. ^b Allocated in comparison with the literature.^{16a}

Upon ring formation, the ^{31}P NMR resonance shifts to lower field (Table 1). Moreover, possible equilibria between **6** and **8** and/or **9** were not observed, which again is in agreement with the theoretical results (**6** \leftrightarrow **8**, $\Delta E[\text{B3LYP}/6\text{-}31\text{G(d)}/\text{PM3}] = 6.5$ kcal/mol; **6** \leftrightarrow **9**, $\Delta E[\text{B3LYP}/6\text{-}31\text{G(d)}/\text{PM3}] = 19.8$ kcal/mol).

By addition of 2 equiv of triphenylphosphane, either **3** or **7** will be formed in an exothermic reaction ($\Delta E[\text{B3LYP}/6\text{-}31\text{G(d)}/\text{PM3}] = -66$ kcal/mol). An azido-tetrazole equilibrium between **3** and **7** is assumed because three ^{31}P NMR signals at $\delta = 21.1$, 16.7, and 15.7 were observed in solution (intensity ratio 5:5:1 (tetrazole/tetrazole/azide); Table 1). In agreement with the experimental finding, theoretical computations suggest an equilibrium because **3** and **7** are only separated by 0.1 kcal/mol (Table 2; cf. $\Delta_{\text{exp}}G_{298} = -0.95$ kcal/mol; $K_{\text{exp}}(298 \text{ K}, \text{CDCl}_3) = 5$). Similar to the equilibrium **2** \leftrightarrow **6**, only the tetrazole isomer **7** and not the open-chain species **3** was found in the solid state.¹¹

The addition of 3 equiv of triphenylphosphane to **1** leads to no further substitution in solution. The triply substituted product **4** can only be obtained by melting **7** with an excess of triphenylphosphane. The third step also represents an exothermic reaction ($\Delta E[\text{B3LYP}/6\text{-}31\text{G(d)}/\text{PM3}] = -53$ kcal/mol). Since quite drastic conditions are required to obtain **4**, a large activation barrier is assumed. The ^{31}P NMR spectrum shows the expected resonance at $\delta = 12.3$. Compound **4** can be regarded as the trimer of Ph_3PNCN ($\delta = 23.1$).¹⁷ The formation of **4** in the solid state was proven by X-ray crystallography and also characterized by NMR, Raman, and IR spectroscopy and mass spectrometry (molecular peak).

Conformational Analysis. Semiempirical calculation at the PM3 level of theory (geometry) and single-point calculations applying density functional theory (energy) were carried out to estimate the stability and thermodynamics of all species in Figure 1. Four of these species [**1**, **4**, **6**, **7**] were isolated and characterized. Since all molecules were derived from **1**, different isomers and conformers have to be considered. For compound **1** there are eight possible conformers. Because of symmetry, there are only two different (nonequivalent) conformations. All conformers with the terminal nitrogen atom of the azide group being in a cis position to the ring C atom were optimized into a trans position, which is in agreement with our experimental

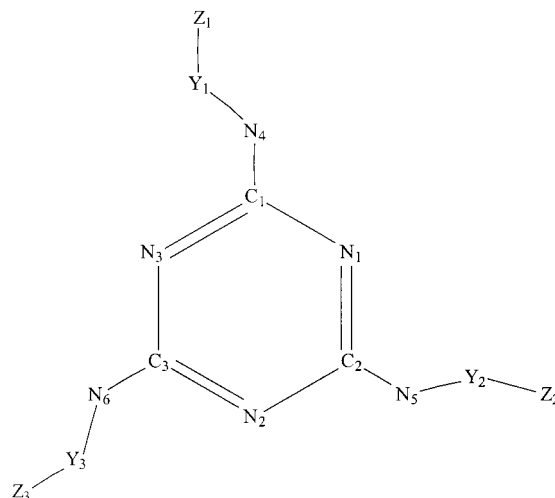


Figure 2. Model for the assignment of the atoms in different species derived from the parent molecule **1**. This arrangement corresponds to ttt (Y1 trans to N1, Y2 trans to N2, Y3 trans to N3; Z1, Z2, and Z3 were always found to be in a trans position to C1, C2, and C3).

results. Therefore, only two conformers were found for **1**. This change from a cis to a trans position of the terminal N atom during the optimization holds for all the considered species. To find a systematic way of assigning all isomers, we have introduced a model that is shown in Figure 2. Table 3 summarizes the results of the conformational analysis.

Tetrazole vs Azide. The azide groups of **2**, **3**, **5**, and **6** are capable of attacking an N atom of the triazine ring, forming a tetrazole ring system (Figure 1). However, in all cases from the electrostatic point of view ring formation should not occur as indicated by the calculated Mulliken partial charges (Table 4). The N atom of the triazine ring and the terminal N atom of the azide possess a large negative charge that should result in a considerable repulsion. The driving force for ring closure can only be explained in terms of a π stabilization of the tetrazole-triazine ring system. These reactions are therefore orbital-controlled and not electrostatically. Moreover, when one PPh_3 group is introduced, the C-N bond system becomes more polarized (ring N atoms possess a larger negative charge, ring C atoms a larger positive charge) and the terminal N atom of the azide group becomes more negative, which should result in a larger repulsion upon ring formation. Introduction of a second PPh_3 group increases this polarization effect and the repulsion between the ring nitrogen and the terminal azide nitrogen atom ($N_{\text{term,azide}}$ vs N_{ring} ; **1**, -0.2676 e vs -0.2900 e; **2**, -0.3258 e vs -0.3408 e; **3**, -0.3594 e vs -0.3815 e; Table 4). However, despite the increased repulsion, ring formation seems to be easier compared to **1** for which no ring formation can be observed. Electron density is transferred into the triazine ring system by the PPh_3 group. Along the molecules **2**–**4** the amount of transferred electron density increases with the number of introduced PPh_3 units [**2**, 0.25 e; **3**, 0.34 e; **4**, 0.40 e].

The charge distribution changes dramatically within the triazine ring system upon ring formation. The nitrogen ring atom attached to the terminal N atom of the azide group now possesses a small positive charge, whereas the ring carbon atom of the tetrazole system (see partial charges of C2 in Table 4) receives a considerable amount of charge to become less positive. This means that electron density is transferred from the cyanuric ring system into the "azide group" of the tetrazole ring system [**5**, 0.40 e; **6**, 0.32 e; **7**, 0.41 e; **8**, 0.21 e]. This charge redistribution seems to be the reason the introduction of

(16) (a) Stefaniak, L.; Roberts, J. D.; Witanowski, M.; Webb, G. A.; Hamdi, B. T. *Org. Magn. Reson.* **1984**, 22 (4), 209. (b) Mason, J. *Multinuclear NMR*; Plenum: New York, 1987. (c) Witanowski, M.; Stefaniak, L.; Januszewski, H. *Nitrogen NMR*; Plenum: London, 1973; p 219. (d) Witanowski, M.; Stefaniak, L.; Januszewski, H. *Annu. Rep. NMR Spectrosc.* **1993**, 25. (e) Hesse, M.; Meier, H.; Zeeh, B. *Spektroskopische Methoden in der Organischen Chemie* (Modern Spectroscopy in Organic Chemistry); Thieme: Stuttgart, 1995.

(17) Ruppert, I.; Appel, R. *Chem. Ber.* **1978**, 111, 751.

Table 3. Relative (kcal/mol) and Absolute Energies (au) (B3LYP/6-31G(d)//PM3)

		equivalent to	$E_{\text{tot}}(\text{B3LYP}/6\text{-}31\text{G}(\text{d})//\text{PM3})$	E_{rel}	
1					
a	ttt	ccc	-771.137 924	0.00	
b	ttc	ctc, tct, cct, ctt, tcc	-771.137 114	0.51	
2^a					
a	ttt	ccc	-1 698.010 963	0.00	
b	ttc	cct	-1 698.007 812	1.98	
c	ctc	ctt	-1 698.009 973	0.62	
d	tcc	tct	-1 698.008 109	1.79	
reaction	1a + PPh ₃ → 2a + N ₂		$\Delta E = -71.8$		
3^b					
a	ttt	ccc	-2 624.874 643	0.00	
b	tcc	ctt	-2 624.871 368	2.06	
c	ttc	ctc	-2 624.870 263	2.75	
d	tct	cct	-2 624.849 263	15.91	
reaction	2a + PPh ₃ → 3a + N ₂		$\Delta E = -65.9$		
4					
a	ttt	ccc	-3 551.717 605	0.00	
b	ttc	ctc, tct, cct, ctt, tcc	-3 551.697 495	12.61	
reaction	3a + PPh ₃ → 4a + N ₂		$\Delta E = -52.9$		
5^a					2a
a	ttt		-1 697.997 036	0.00	8.74
b	ttc		-1 697.989 618	4.76	13.39
c	ctc		-1 697.989 452	4.65	13.50
d	ctt		-1 697.993 354	2.31	11.05
6^a					2a
a	ccc		-1 698.008 867	0.00	1.31
b	tcc		-1 698.006 438	1.52	2.84
c	tct		-1 697.998 893	6.26	7.57
d	cct		-1 697.998 575	6.46	7.77
7^c					3a
a	ttt	ccc	-2 624.874 517	0.00	0.08
b	tcc	ttc	-2 624.841 054	16.37	16.45
c	ctc	tct	-2 624.853 988	12.88	12.96
8^{d,e}					2a
	ttt	ccc	-1 697.998 572		7.78
9^d					2a
	ttc	ctc	-1 697.977 253		21.15

^a Azide groups attached to C1, NPPH₃ attached to C3. ^b Azide group attached to C1. ^c NPPH₃ attached to C1 and C3; ttc (ctc) does not represent a stable isomer and is optimized to ttt. ^d NPPH₃ attached to C1. ^e The conformer ctt (which is equivalent to tcc) does not possess a minimum.

Table 4. Mulliken Partial Charges (in e)^a

	C1	N1	C2	N2	C3	N3	N4	N5	N6	Y1	Y2	Y3	Z1	Z2	Z3
(1)ttt	+0.2245	-0.2900	+0.2245	-0.2900	+0.2245	-0.2900	-0.4175	-0.4175	-0.4175	+0.7505	+0.7505	+0.7505	-0.2676	-0.2676	-0.2676
(2)ttt	+0.2253	-0.3408	+0.2253	-0.3584	+0.2816	-0.3515	-0.4317	-0.4441	-0.7427	+0.7679	+0.7680	+2.2313	-0.3258	-0.3202	-0.5844
(3)ttt	+0.2280	-0.4009	+0.2828	-0.4193	+0.2851	-0.3815	-0.4523	-0.7609	-0.7514	+0.7795	+2.1917	+2.1965	-0.3594	-0.5786	-0.5781
(4)ttt	+0.2978	-0.4509	+0.2861	-0.4409	+0.2789	-0.4410	-0.7761	-0.7634	-0.7726	+2.1666	+2.1743	+2.1798	-0.5938	-0.5862	-0.5896
(5)ttt	+0.1664	+0.1019	+0.0169	+0.1019	+0.2679	-0.2875	-0.4221	-0.2262	-0.7334	+0.7644	+0.0594	+2.2532	-0.2801	-0.1722	-0.5921
(6)ccc	+0.2309	-0.2847	-0.0158	+0.0981	+0.2512	-0.3721	-0.4389	-0.1835	-0.7514	+0.7613	+0.0297	+2.3034	-0.3020	-0.1628	-0.6076
(7)ttt	+0.2458	+0.0855	+0.0191	-0.3853	+0.2834	-0.3998	-0.7680	-0.2475	-0.7450	+2.2635	+0.0311	+2.2051	-0.5912	-0.1892	-0.6031
(8)ttt	+0.2384	+0.1358	-0.1285	+0.1709	-0.0125	-0.3203	-0.7527	-0.1123	-0.1889	+2.3220	+0.0127	+0.0390	-0.6132	-0.1132	-0.1408
(9)ttc	+0.2608	+0.0525	-0.0148	-0.0988	+0.0292	+0.0009	-0.7576	-0.1802	-0.2161	+2.4227	+0.0545	+0.1149	-0.6354	-0.1762	-0.3487

^a See Figure 2.

the PPh₃ groups is so important for ring closure and explains why the remaining C–N bonds become more strongly polarized.

To gain further insight into the thermodynamics and the kinetics of the **2** ↔ **6** and **3** ↔ **7** equilibria as well as the influence of the PPh₃ groups, we performed calculations on the model compound **1** at the B3LYP/6-31G(d) level (full optimization). The calculated structures of different isomers of **1** and possible cyclization products are depicted in Figure 3. Two different structures were found for **1**, **TR1**, and **TR2**. All structures are planar and represent minima on the potential energy surface. The azide groups lie in the ring plane that favors the delocalization of the π electron density over the entire species.¹⁸ The most relevant changes upon cyclization are the bending of the azide group of around 58° and the increase of

the terminal N–N distance of the azide group of around 0.16 Å. These changes reveal the magnitude of the electron density redistribution, which was examined in detail above. Remarkably, all structures derived from **1a** (**TR1a** and **TR2a**) are more stable than those derived from **1b** (**TR1b** and **TR2b**; Table 5).

For **1** it is known that no cyclization has been experimentally observed.¹⁹ Such a cyclization would result in formation of **TR1a** or **TR1b** (Table 5, Figure 3). In contrast to the **2** ↔ **6** and **3** ↔ **7** equilibria, all possible cyclization reactions (**1a** ↔ **TR1a**, **TR1a** ↔ **TR2a**, and **TR2a** ↔ **TR3**) of **1** were calculated

(18) Zhaoxu, C.; Jianfen, F.; Heming, X. *J. Mol. Struct.: THEOCHEM* **1999**, *458*, 249.

(19) Kessenich, E. Diploma Thesis, Ludwig-Maximilians-Universität München, Munich, Germany, 1997.

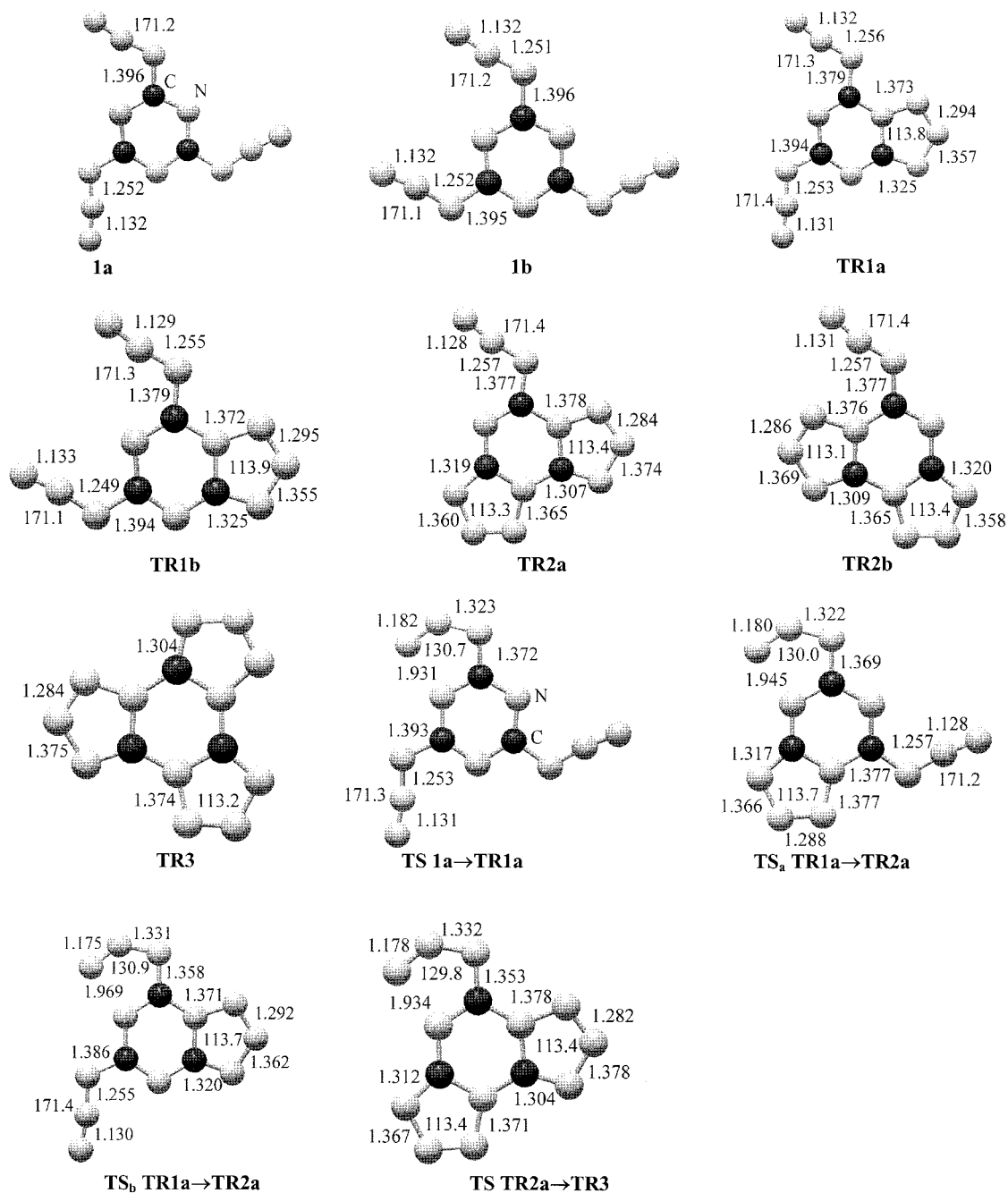


Figure 3. B3LYP/6-31G(d) fully optimized geometries of different isomers of **1** and the transition states for the cyclization (distances in Å, angles in deg).

to be endothermic by 8–11 kcal/mol and possess equilibrium constants of around 10^{-8} – 10^{-11} (Table 5). Approximations of the equilibrium constants of the $2 \leftrightarrow 6$ and $3 \leftrightarrow 7$ equilibria and the Gibbs free energies were determined by integration of suitable NMR signals. The experimental equilibrium constants of 2.6 for the $2 \leftrightarrow 6$ and 5.0 for the $3 \leftrightarrow 7$ equilibria are nicely in agreement with the calculated values of 0.1 and 0.9 (B3LYP/6-31G(d)/PM3, Table 5), respectively.^{12,13} The B3LYP/6-31G(d) (full optimization) result of 1.5 for the $2 \leftrightarrow 6$ equilibrium constant shows a smaller deviation from experimental results. Unfortunately, this level of theory is not feasible for larger systems such as **3**, **4**, and **7**. The huge difference between the equilibrium constants of the $1a \leftrightarrow TR1a$ and $2 \leftrightarrow 6$ ($3 \leftrightarrow 7$) equilibria nicely explains the influence of the PPH₃ group as a tetrazole-stabilizing group with respect to thermodynamics.

Electron-donating groups such as PPH₃ enhance ring closure and stabilize the tetrazole form.²⁰

In the next step the activation barrier for the cyclization was investigated.²¹ There are several factors leading to activation barriers for this type of 1,5-dipolar cyclization: (i) the unfavorable charge distribution (electrostatic repulsion, Table 4) with a negatively charged terminal azide and ring nitrogen atom, (ii) the bending of the N–N–N angle in the azide (from 171 to 113°, Figure 3), and (iii) a charge redistribution upon ring closure. In accordance with this, all three cyclization steps,

(20) (a) Butler, R. N.; Scott, F. L. *J. Org. Chem.* **1966**, *31*, 3182. (b) Lieber, E.; Sherman, E.; Henry, R. A.; Cohen, J. *J. Am. Chem. Soc.* **1951**, *73*, 23. (c) Norris, W. P.; Henry, R. A. *J. Org. Chem.* **1964**, *29*, 650. (d) Henry, R. A.; Finnegan, W. G.; Lieber, E. *J. Am. Chem. Soc.* **1955**, *77*, 2265.

(21) Schulz, A. *Trends Inorg. Chem.* **1999**, *6*, 137.

Table 5. Absolute (au) and Relative (kcal/mol) Energies of **1**, **2a**, **6a**, and **6b** Fully Optimized at B3LYP/6-31G(d)^a

	E^{tot}	ΔE	ΔH_{298}	ΔG_{298}		K
1a	-771.159 322	0.00	0.00	0.00		
1b	-771.158 509	0.51	0.49	0.46		
TR1a	-771.142 372	10.64	10.74	12.30	1a → TR1a :	6×10^{-10}
TR1b	-771.140 411	11.87	11.92	13.45	1b → TR1b :	2×10^{-10}
TR2a	-771.129 014 5	18.51	18.80	21.92	TR1a → TR2a :	6×10^{-8}
TR2b	-771.123 252	22.63	22.73	25.69	TR1b → TR2b :	7×10^{-10}
TR3	-771.112 673	29.27	29.61	34.15	TR2a → TR3 :	7×10^{-10}
TS	1a → TR1a	-771.121 032	24.03	22.82	24.21	
TS_a	TR1a → TR2a^b	-771.105 029	34.07	33.01	35.93	
TS_b	TR1a → TR2a^b	-771.107 560	32.48	31.41	34.40	
TS	TR2a → TR3	-771.091 874	41.81	40.89	45.42	
2a^c	-1 697.982 960	0.00				
6a^c	-1 697.983 364	-0.25		-0.57 ^d	2a → 6a :	1.5 ^e
6b^c	-1 697.981 348	1.01			2a → 6b :	0.2 ^e
TS2a-6a^c	-1 697.949 500	19.98				

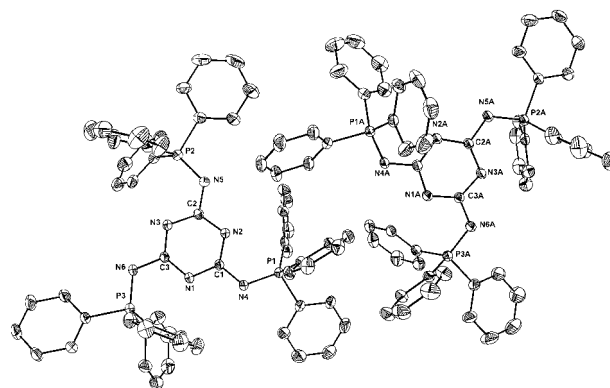
^a See Figure 3. ^b There are two possible ways to form **TR2a** resulting in two different transition states; see Figure 3. ^c See Table 2, Figure 1. ^d Experimental value (derived from ³¹P NMR data; this work). ^e cf., $K_{\text{exp}} = 2.7$; see ref 13.

finally resulting in **TR3**, are calculated to possess fairly large activation barriers to cyclization with 23 (formation of the first tetrazole ring, **TR1a**), 21 (formation of the second tetrazole ring, **TR2a**), and 18 (formation of the third tetrazole ring, **TR3**) kcal/mol. Introduction of a PPh₃ group slightly decreases the activation barrier to 20 kcal/mol (**2a** ↔ **6a** isomerization). There is no experimental data directly available for comparison, but the activation energies for related reactions agree well. For example, an activation barrier of 19.2 kcal/mol for the ring opening of 1-(*p*-chlorophenyl)pentazole in CD₃OD/CD₂Cl₂ in the temperature range from -10 to 0 °C was found that compares well with our results.²² More recently, ab initio calculations of the isomerization of azido and tetrazole forms of thiazole[3,2-*d*]tetrazole were reported. In agreement with our results a transition state was found being around 19 kcal/mol higher in energy compared to the energies of both isomers. The tetrazole structure was estimated to be less stable by 1.2 kcal/mol.⁷ It should be noted that polar solvents may have a considerable influence on the activation barrier. For the thiazole-[3,2-*d*]tetrazole system it was found that the free energy barrier is not drastically changed upon solvation (~1 kcal/mol in water), suggesting little variations in the kinetics.⁷

The geometries of the different transition states for the cyclization of **1** are shown in Figure 3 and display strongly distorted azide groups with N_{ring}-N_{azide} distances between 1.931 and 1.945 Å and N-N-N angles between 129.8° and 130.7°. As expected, the optimized parameters for the transition states are between those of the azides and tetrazoles. Interestingly, there are two different transition states (**TS_a** and **TS_b**, **TR1a** → **TR2a**, Figure 3) describing the cyclization of **TR1a** that results in the formation of **TR2a**. Since in **TR1a** there are two nonequivalent azide groups capable of forming a tetrazole ring, two different reaction paths are possible. **TS_a** was found to be 1.6 kcal/mol less stable than **TS_b**, **TR1a** → **TR2a**.

Crystallography. The crystallographic data and refinement details for compounds **4** and **6** are summarized in the Experimental Section. Single crystals of **6** suitable for X-ray structure determination were obtained by recrystallization from dichloroethane at ambient temperature, and crystals of **4** were obtained by recrystallization from xylene. Selected bond lengths [Å] and angles [deg] for **4** and **6** are given in Tables 6 and 7.

2,4,6-Tris(triphenylphosphanimino)-1,3,5-triazazine (**4**) crystallizes in the triclinic space group *P*1̄ with four molecules in the

**Figure 4.** ORTEP drawing of **4**. Thermal ellipsoids with 25% probability at 293 K (hydrogen atoms omitted).**Table 6.** Selected Bond Lengths [Å] and Angles [deg] for **4**

P(1)-N(4)	1.588(3)	P(1A)-N(4A)	1.585(3)
N(4)-C(1)	1.360(4)	N(4A)-C(1A)	1.367(4)
C(1)-N(2)	1.347(4)	C(1A)-N(2A)	1.349(4)
N(2)-C(2)	1.347(4)	N(2A)-C(2A)	1.348(4)
P(1)-N(4)-C(1)	120.8(2)	P(1A)-N(4A)-C(1A)	121.5(3)
P(2)-N(5)-C(2)	124.8(3)	P(2A)-N(5A)-C(2A)	119.4(3)
P(3)-N(6)-C(3)	115.8(2)	P(3A)-N(6A)-C(3A)	122.7(2)
N(4)-C(1)-N(2)	120.6(3)	N(4A)-C(1A)-N(2A)	120.0(3)
C(1)-N(2)-C(2)	115.4(3)	C(1A)-N(2A)-C(2A)	115.3(3)

Table 7. Selected Bond Lengths [Å] and Angles [deg] for **6**

P(1)-N(1)	1.611(4)	P(1a)-N(1a)	1.624(4)
N(1)-C(19)	1.308(6)	N(1a)-C(19a)	1.310(6)
N(10)-N(9)	1.098(9)	N(10a)-N(9a)	1.099(6)
N(9)-N(8)	1.224(9)	N(9a)-N(8a)	1.230(7)
N(8)-C(20)	1.374(9)	N(8a)-C(20a)	1.397(7)
C(20)-N(3)	1.306(8)	C(20a)-N(3a)	1.309(7)
N(3)-C(21)	1.332(9)	N(3a)-C(21a)	1.334(7)
C(21)-N(4)	1.309(9)	C(21a)-N(4a)	1.314(7)
N(4)-N(5)	1.361(9)	N(4a)-N(5a)	1.364(7)
N(5)-N(6)	1.313(7)	N(5a)-N(6a)	1.318(6)
N(6)-N(7)	1.362(7)	N(6a)-N(7a)	1.359(6)
N(10)-N(9)-N(8)	170.6(7)	N(10a)-N(9a)-N(8a)	170.3(5)
N(4)-N(5)-N(6)	112.3(6)	N(4a)-N(5a)-N(6a)	113.0(5)
P(1)-N(1)-C(19)	125.6(4)	P(1a)-N(1a)-C(19a)	121.1(3)

unit cell. The perspective view of **4** is shown in Figure 4. In agreement with our computation, the molecule crystallizes in a trans and a cis configuration (Figures 2 and 4), which are equivalent and can be transformed into each other by a 180° rotation about the N2-C5 axis. An angle of 9° is found between the two planar triazine ring systems.

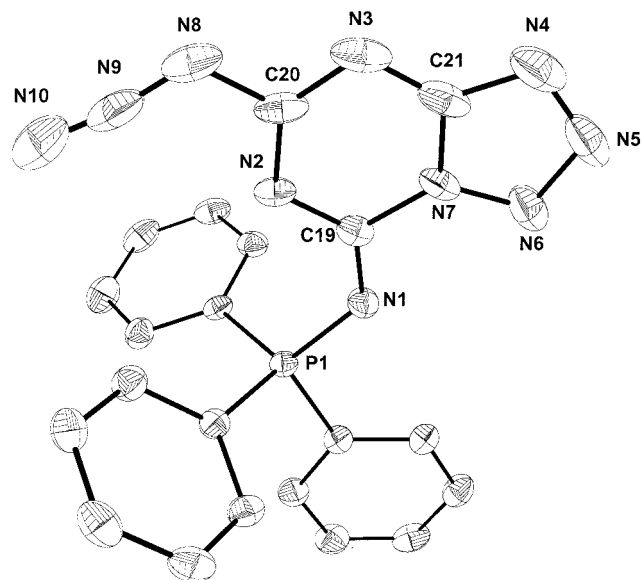


Figure 5. ORTEP drawing of **6**. Thermal ellipsoids with 25% probability at 293 K (hydrogen atoms omitted).

The P–N bond length of about 1.59 Å corresponds to a bond order between 1 and 2, indicating π character in the P–N bonds. P–N–C angles between 116° and 125° are found that are comparable with the P–N–C angle of about 122° observed in the monomeric species (Ph₃PNCN).²³

2-Triphenylphosphanimino-4-azidotetrazolo[5,1-*a*]-[1,3,5]triazine (**6**) crystallizes in the monoclinic space group *C2/c* with eight molecules and four solvent molecules in the unit cell. The molecular structure of compound **6** is shown in Figure 5. By use of our model according to Figure 2, the molecule crystallizes in the trans–cis–cis conformation, which does not represent the lowest-lying isomer. According to our calculation the cis–cis–cis arrangement should be slightly favored. However, the trans–cis–cis conformation is only 1.5 kcal/mol (B3LYP/6-31G(d)//PM3, gas phase) less stable. Thus, Coulomb and packing forces could be responsible for the observed trans–cis–cis molecular structure of **6** in the solid state.^{12,13}

The P–N distances in **6** are 1.611 and 1.625 Å, which are significantly longer than the P–N distances in **4**. These values also correspond to a bond order between 1 and 2. In comparison, the sum of the covalent radii (PN) is 1.8 Å for a single P–N bond and 1.6 Å for a double bond.²⁴ A typical P–N bond with π character is found in R₃–P=N–R compounds with 1.602 Å.²⁵ The bond lengths and angles of the tetrazole ring also agree with the data found in the literature.²⁶

Conclusion

All three steps of the reaction 2,4,6-triazido-1,3,5-triazine with triphenylphosphane represent exothermic reactions. For the species **2** and **3** only, the reaction in solution results in observable equilibria between a tetrazole and an open azide chain isomer. The energy difference between these two isomers is very small and was estimated to be about ± 1 kcal/mol. In the solid state only the tetrazole species were observed and characterized by X-ray crystallography.

The experimental observation of an azide–tetrazole equilibrium **2** \leftrightarrow **6** and **3** \leftrightarrow **7**, in contrast to **1** \leftrightarrow **TR1**, can be explained with the thermodynamic stabilization of the tetrazole isomer due to the introduction of the PPh₃ group. The fairly large activation barrier to cyclization of about 20–25 kcal/mol may be partly attributed to an unfavorable electrostatic repulsion between the terminal nitrogen atom of the azide group and the ring nitrogen atoms as well as to the bending of the azide group.

The introduction of PPh₃ groups results in more strongly polarized C–N ring bonds and in a charge transfer into the triazine ring system. The orbital-controlled ring formation is accompanied by a considerably large charge transfer into the tetrazole ring system and therefore thermodynamically stabilizes the tetrazole isomer. This redistribution may explain the importance of the PPh₃ groups because they represent good electron donors.

Experimental Section

General Remarks. CAUTION! 2,4,6-Triazido-1,3,5-triazine is highly shock-sensitive and a powerful explosive! The explosive nature increases with greater purity and crystal size. This compound should be handled only on a millimolar scale using appropriate safety precautions, i.e., face shields, leather gloves, protective jackets, and safety shields. Plastic beakers and spatulas should be used during the preparation.

Solvents were freshly distilled, dried, and stored under nitrogen. NMR: JEOL Eclipse 400/GSX 270 Delta (¹H, ¹³C chemical shifts refer to $\delta_{\text{TMS}} = 0.00$; ¹⁵N to $\delta_{\text{CH}_3\text{NO}_2} = 0.00$; ³¹P to $\delta_{\text{H}_3\text{PO}_4(85\%)} = 0.00$). IR: Nicolet 520 FT-IR (as KBr pellets or in Nujol mulls between KBr windows). Raman: Perkin-Elmer Spectrum 2000R NIR FT. CHN analyses: Analysator Elementar Vario EL. MS: Finnigan MAT 90. Melting points are uncorrected (Büchi B540). 2,4,6-Triazido-1,3,5-triazine was prepared according to the procedure given in the literature.²

2,4,6-Tris(triphenylphosphanimino)-1,3,5-triazine (4). **4** was prepared according to the literature.^{3b} C₅₇H₄₅N₆P₃ (906.9) yield: 99%, colorless crystals, mp 239 °C. IR (KBr): $\tilde{\nu}$ (cm⁻¹) = 3048 (w, CH), 1589 (vw, CC), 1575 (vw, CC), 1472 (vs), 1436 (s), 1364 (s, br), 1311 (w), 1287 (vw), 1275 (vw), 1179 (m), 1158 (m), 1111 (s), 1071 (vw), 1029 (vw), 998 (vw), 894 (w), 823 (m), 748 (w), 717 (s), 692 (s), 615 (vw), 532 (s), 524 (s). Raman (100 mW): $\tilde{\nu}$ (cm⁻¹) = 3058 (7.5, CH), 1590 (5.0, CC), 1574 (2.0, CC), 1492 (1.0), 1439 (0.5), 1376 (1.0), 1214 (1.0), 1187 (1.0), 1162 (1.0), 1113 (2.5), 1032 (2.0), 1000 (10), 899 (0.5), 691 (0.5), 618 (1.5), 583 (1.5), 254 (1.5). ¹H NMR (CDCl₃): $\delta = 8-7.3$ (m, 45 H, C₆H₅). ¹³C NMR (CDCl₃): $\delta = 171$ (br, C_{triazine}), 133–127 (54 C, C_{phenyl}). ³¹P NMR (CDCl₃): $\delta = 12.3$ (s). MS (EI, 70 eV), *m/z* (%): 907 (26) [M⁺], 906 (63) [M⁺ – H], 302 (50) [PPh₃NCN⁺], 301 (100.0) [PPh₃NCN⁺ – H], 288 (6) [PPh₃NC⁺], 277 (69) [PPh₃NH⁺], 262 (79) [PPh₃⁺], 185 (28) [PPh₂⁺], 183 (87) [PPh₂⁺ – H₂], 152 (17) [Ph₂⁺ – H₂], 108 (25) [PPh⁺], 77 (35) [Ph⁺]. C₅₇H₄₅N₆P₃ (906.95) calcd: C 75.49, H 5.00, N 9.27. Found: C 75.28, H 5.10, N 9.23.

2-Triphenylphosphanimino-4-azidotetrazolo[5,1-*a*]-[1,3,5]triazine (6). Into a solution of 0.5 g (2.45 mmol) of **1** in anhydrous ether, a solution of 0.7 g (2.65 mmol) of PPh₃ was added during a period of 2 h at ambient temperature. The solution was filtered and recrystallized from dichloroethane. C₂₁H₁₅N₁₀P (438.1) yield: 99%, colorless crystals, mp 195 °C (dec). IR (KBr): $\tilde{\nu}$ (cm⁻¹) = 3058 (w, CH), 2153 (m, $\nu_{\text{as}}(\text{N}_3)$), 1601 (s, CC), 1574 (m), 1539 (s, CC), 1499 (m), 1484 (m), 1454 (s), 1435 (s), 1335 (m), 1320 (m), 1297 (m), 1270 (w), 1230 (w), 1222 (w), 1192 (w), 1188 (w), 1161 (vw), 1156 (vw), 1114 (m), 1088 (vw), 1073 (vw), 1030 (vw), 1012 (vw), 997 (vw), 980 (vw), 912 (w), 886 (w), 789 (w), 783 (vw), 745 (w), 724 (m), 692 (m), 581 (w), 552 (w), 532 (s), 519 (m), 511 (w), 490 (vw). Raman (100 mW): $\tilde{\nu}$ (cm⁻¹) = 3063 (9.2, CH), 2146 (0.5, $\nu_{\text{as}}(\text{N}_3)$), 1590 (4.5, CC), 1190 (1.5, $\nu_{\text{s}}(\text{N}_3)$), 1002 (10, phenyl). ¹H NMR (CDCl₃, 270 MHz, 25 °C): $\delta = 8-7.3$ (m, 15 H, C₆H₅). ¹³C NMR ([D₆]DMSO): $\delta = 162.9$ (d, ⁴J_{CP} = 1.5 Hz, C20), 158.5 (d, ⁴J_{CP} = 1.5 Hz, C21), 151.6 (d, ²J_{CP} = 1.6 Hz, C19), 133.7 (d, ⁴J_{CP} = 3.0 Hz, 3 C, C_{phenyl}), 132.9 (d, ³J_{CP} = 10.8 Hz, 6 C, C_{phenyl}), 129.3 (d, ²J_{CP} = 13.0 Hz, 6 C, C_{phenyl}), 124.5 (d, ¹J_{CP}}}}}}}}

(23) Kaiser, J.; Hartung, H.; Richter, R. *Z. Anorg. Allg. Chem.* **1980**, 469, 188.

(24) Campana, C. F.; Lo, F. Y.-K.; Dahl, L. F. *Inorg. Chem.* **1979**, 18, 3060.

(25) Dehnicke, K.; Weller, F. *Coord. Chem. Rev.* **1997**, 158, 103–169.

(26) Palenik, G. J. *Acta Crystallogr.* **1963**, 16, 596.

= 102.6 Hz, 3 C, C_{phenyl}). ¹⁵N NMR ([D₆]DMSO, 40.57 MHz, 25 °C): δ = 17.0 (s, N5), -35.1 (s, N6), -79.1 (s, N4), -142.5 (s, N_{azide}), -144.2 (s, N_{azide}), -151.1 (d, ³J_{NP} = 11.2 Hz, N7), -181.2 (d, ³J_{NP} = 6.5 Hz, N2), -192.4 (s, N3), -265.4 (s, N8), -266.3 (d, ¹J_{NP} = 32.5 Hz, N1). ³¹P NMR ([D₆]DMSO): δ = 24.7 (s, P). MS (EI, 70 eV), *m/z* (%): 438 (100) [M⁺], 412 (30) [M⁺ - CN], 386 (52) [M⁺ - C₂N₂], 302 (29) [PPh₃NCN⁺], 301 (65) [PPh₃NCN⁺ - H], 262 (27) [PPh₃⁺], 185 (43) [PPh₂⁺], 108 (16) [PPh⁺], 77 (7) [Ph⁺]. C₂₁H₁₅N₁₀P₁ (438.4) calcd: C 57.54, H 3.45, N 31.95. Found: C 57.6, H 3.3, N 31.4.

Crystal Structure Analysis of 4. C₅₇H₄₅N₆P₃, MW = 906.90, crystal size: 0.53 mm × 0.37 mm × 0.17 mm, transparent plate, anorthic, space group *P*1̄, *a* = 14.705(3) Å, *b* = 17.705(4) Å, *c* = 21.528(3) Å, α = 108.99(2)°, β = 91.612(13)°, γ = 111.66(2)°, *V* = 4855(2) Å³, *Z* = 4, *d*_{calcd} = 1.241 Mg/m³, μ = 0.167 mm⁻¹, *F*(000) = 1896. Nonius Mach3, ω scan, Mo Kα, λ = 0.710 73 Å, *T* = 293(2) K, 2θ range = 2.28–23.98° in -16 ≤ *h* ≤ 16, -19 ≤ *k* ≤ 20, -24 ≤ *l* ≤ 0, reflections collected 15 650, independent reflections 15 185 (*R*_{int} = 0.0219), observed reflections 10 676 (*I* > 2σ(*I*)). Structure solution program: SHELXS-86 (G. M. Sheldrick, University of Göttingen, Germany, 1986), direct methods. Final *R* indices [*I* > 2σ(*I*): *R*1 = 0.0636, w*R*2 = 0.1434, *R*1 = 0.0968, w*R*2 = 0.1637 (all data), GOF on *F*² = 1.026, 865 refined parameters, largest difference peak/hole 0.664, -0.417 e Å⁻³. Program used: SHELXL-93 (G. M. Sheldrick, University of Göttingen, Germany, 1993).

Crystal Structure Analysis of 6. C₂₁H₁₅N₁₀P₁·0.5 C₂H₄Cl₂, MW = 487.87, crystal size: 0.2 mm × 0.47 mm × 0.53 mm, colorless plate, monoclinic, space group *C*2/*c*, *a* = 42.059(6) Å, *b* = 13.916(4) Å, *c* = 15.995(4) Å, β = 101.77(2)°, *V* = 9165(4) Å³, *Z* = 8, *d*_{calcd} = 1.414 Mg/m³, μ = 0.270 mm⁻¹, *F*(000) = 4016. Nonius Mach3, ω scan, Mo Kα, λ = 0.710 73 Å, *T* = 293(2) K, 2θ range = 2.59–23.98° in -48 ≤ *h* ≤ 0, 0 ≤ *k* ≤ 15, -17 ≤ *l* ≤ 18, reflections collected 7275, independent reflections 7168 (*R*_{int} = 0.0201), observed reflections 4342 (*I* > 2σ(*I*)). Structure solution program: see 4, direct methods. Final *R* indices [*I* > 2σ(*I*): *R*1 = 0.0758, w*R*2 = 0.1632, *R*1 = 0.1293, w*R*2 = 0.1946 (all data), GOF on *F*² = 1.016, 505 refined parameters, largest difference peak/hole 0.440, -0.445 e Å⁻³. Program used: see 4.

Computational Methods

The computations were carried out at the semiempirical PM3 level (full optimization), and all species were characterized as minima by a frequency analysis. At the DFT level only single points (using the optimized PM3 structure, notation B3LYP/6-31G(d)//PM3) were calculated to obtain more reliable energies. To check this procedure, calculations were carried out on the model compound **1** as well as on the species **2a** and **6a** using the B3LYP/6-31G(d) method (full optimization). All energies are summarized in Tables 3 and 4. The agreement between the B3LYP single-point values and the fully optimized values is very good. It is not feasible to carry out all optimizations using the B3LYP/6-31G(d) method.

The energies at the B3LYP/6-31G(d)//PM3 level are not temperature-corrected. Temperature correction was only possible at the fully optimized B3LYP/6-31G(d) level for the isomers of **1**.¹³ The thermodynamics in a vacuum was computed by correcting the differences in the electronic energies to enthalpies at 298 K upon inclusion of zero-point energy and thermal corrections. The free energy differences were estimated from the addition of entropic corrections. All these terms were determined with the harmonic oscillator—rigid rotor approximation from the optimized geometries.²⁷

The hybrid method B3LYP includes a mixture of Hartree–Fock exchange with DFT exchange–correlation. Becke’s three-parameter functional where the nonlocal correlation is provided by the LYP expression (Lee, Yang, Parr correlation functional) was used, which is implemented in Gaussian 98.²⁸ For a concise definition of the B3LYP functional see ref 29.

It should be emphasized that the computation was carried out for a single, isolated (gas-phase) molecule. There may well be significant differences among gas-phase, solution, and solid-state data.

Acknowledgment. A.S. thanks Prof. Dr. T. M. Klapötke (LMU München) for his generous support and advice. We also wish to thank the Leibniz Rechenzentrum for a generous allocation of CPU-time. We are indebted to and thank both reviewers for most valuable comments and suggestions.

Supporting Information Available: X-ray crystallographic files, in CIF format, for the structure determinations of **4** and **6**; the fully optimized structural and spectroscopic data of **1a**, **1b**, **TR2a**, **TR2b**, **TR3**, and all transition states. This material is available free of charge via the Internet at <http://pubs.acs.org>.

IC000526K

- (27) McQuerrrie, D. *Statistical Mechanics*; Harper & Brown: New York, 1976.
- (28) Frisch, M. J.; Trucks, G. W.; Schlegel, H. B.; Scuseria, G. E.; Robb, M. A.; Cheeseman, J. R.; Zakrzewski, V. G.; Montgomery, J. A., Jr.; Stratmann, R. E.; Burant, J. C.; Dapprich, S.; Millam, J. M.; Daniels, A. D.; Kudin, K. N.; Strain, M. C.; Farkas, O.; Tomasi, J.; Barone, V.; Cossi, M.; Cammi, R.; Mennucci, B.; Pomelli, C.; Adamo, C.; Clifford, S.; Ochterski, J.; Petersson, G. A.; Ayala, P. Y.; Cui, Q.; Morokuma, K.; Malick, D. K.; Rabuck, A. D.; Raghavachari, K.; Foresman, J. B.; Cioslowski, J.; Ortiz, J. V.; Stefanov, B. B.; Liu, G.; Liashenko, A.; Piskorz, P.; Komaromi, I.; Gomperts, R.; Martin, R. L.; Fox, D. J.; Keith, T.; Al-Laham, M. A.; Peng, C. Y.; Nanayakkara, A.; Gonzalez, C.; Challacombe, M.; Gill, P. M. W.; Johnson, B. G.; Chen, W.; Wong, M. W.; Andres, J. L.; Head-Gordon, M.; Replogle, E. S.; Pople, J. A. *Gaussian 98*, revision A.6; Gaussian, Inc.: Pittsburgh, PA, 1998.
- (29) (a) Bauschlicher, C. W.; Partridge, H. *Chem. Phys. Lett.* **1994**, *231*, 277. (b) Becke, A. D. *J. Chem. Phys.* **1993**, *98*, 5648. (c) Becke, A. D. *Phys. Rev. A* **1988**, *38*, 3098. (d) Lee, C.; Yang, W.; Parr, R. G. *Phys. Rev. B* **1988**, *37*, 785. (e) Vosko, S. H.; Wilk, L.; Nusair, M. *Can. J. Phys.* **1980**, *58*, 1200.